

# Effects of thermal treatment on injectability and basic properties of apatite cement containing spherical tetracalcium phosphate made with plasma melting method

Kunio ISHIKAWA,\* Akari TAKEUCHI,\* Yumiko SUZUKI\*,\*\* and Kiyoshi KOYANO\*\*

\*Department of Biomaterials, Faculty of Dental Science, Kyushu University, 3-1-1 Maidashi, Higashiku, Fukuoka 812-8582

\*\*Department of Removable Prosthodontics, Faculty of Dental Science, Kyushu University, 3-1-1 Maidashi, Higashiku, Fukuoka 812-8582

We have previously prepared spherical-shaped tetracalcium phosphate (s-TTCP) with plasma melting method. We found that apatite cement (AC) containing s-TTCP showed excellent injectability from syringe and handling property when compared with AC that contained irregular-shaped TTCP (i-TTCP). However, transformation of AC containing s-TTCP (s-AC) to apatitic mineral was suppressed and thus mechanical strength of set s-AC was low. In the present study, thermal treatment was attempted on s-TTCP to convert heat decomposition products formed in s-TTCP during plasma melting process to TTCP. X-ray diffraction (XRD) analysis revealed that some heat decomposition products in s-TTCP converted to TTCP when s-TTCP was heated at 1,500°C for four hours and quenched at room temperature (q-TTCP). AC containing q-TTCP transformed to apatitic monolith and showed equivalent mechanical strength similar to AC that contained i-TTCP—without sacrificing excellent injectability from syringe and handling property. Based on these findings, we concluded that AC containing q-TTCP would benefit patients since it delivered excellent injectability without sacrificing basic setting properties of AC.

Key-words: Apatite cement, Calcium phosphate cement, Injectability, Tetracalcium phosphate, Spherical powder

[Received October 10, 2007; Accepted November 15, 2007] ©2008 The Ceramic Society of Japan

## 1. Introduction

Apatite cement (AC) has dramatically changed the surgical landscape for the reconstruction of bone defects because of its two favorable characteristics: injectability and high mechanical strength upon transformation to apatite monolith. Injectable AC permits minimally invasive surgical operations.<sup>1-3)</sup> For example, injection of AC to a deformed condyle through syringe results in expansion of the condyle without open surgery. In terms of mechanical strength, apatite monolith is formed upon setting when powder phase of apatite cement is mixed with its liquid phase. Although many types of AC have been reported to date,<sup>4-22)</sup> the setting mechanism of all ACs is basically the same. In other words, powder phase of AC dissolves to supply calcium and phosphate ions, and the ions reprecipitate as hydroxyapatite (HAP:  $\text{Ca}_{10}(\text{PO}_4)_6(\text{OH})_2$ ) since HAP is the most stable phase thermodynamically at neutral and basic pH regions.<sup>14)</sup> Precipitated HAP crystals then interlock each other to form apatite monolith. Since the key role of the powder phase of AC is to supply calcium and phosphate ions, shape of the powder phase is less important if the rate of calcium and phosphate ions supply can be adjusted.

On the other hand, shape of powder phase strongly influences injectability. In particular, spherical-shaped powder is easy to be injected from the syringe when compared with irregular-shaped powder—if diameter of powder particles is the same. We have previously prepared spherical-shaped tetracalcium phosphate (s-TTCP;  $\text{Ca}_4(\text{PO}_4)_2\text{O}$ ) with plasma melting method to produce AC by mixing s-TTCP with dicalcium phosphate anhydrous (DCPA;  $\text{CaHPO}_4$ ).<sup>20)</sup> This s-TTCP-DCPA based AC shall be referred to as s-AC hereinafter. The s-AC showed much

better injectability when compared with ordinary AC or irregular AC (i-AC) which contains irregular-shaped TTCP (i-TTCP) and DCPA.<sup>20)</sup> For example, load required to dispense  $0.02 \text{ cm}^{-3}$  of conventional apatite cement (c-AC) paste from 18 G syringe needle at a rate of  $1 \text{ cm}^3 \cdot \text{min}^{-1}$  was 2400 g. On the other hand, only 190 g was required to dispense s-AC paste from the same syringe at the same rate. The s-AC also possesses better handling property. Cement spread area used as an index of handling property was  $158 \text{ mm}^2$  when a 2 kg glass was placed on 0.2 mL of c-AC paste. In contrast, cement spread area for s-AC was as large as  $512 \text{ mm}^2$ .

These findings indicated that s-AC is a promising AC candidate. Unfortunately, we found that transformation of s-AC to apatite was limited and thus mechanical strength of set s-AC was low. Although the detailed mechanism of limited transformation of s-AC to apatitic mineral has not been clarified, it is obvious that s-TTCP caused these problems since the only difference between i-AC and s-AC is s-TTCP. In addition, we found that an unidentified product was formed during the preparation of s-TTCP using plasma melting method. Since there are many methods to prepare spherical TTCP, one way to circumvent the formation of unexpected or unidentified products is to prepare spherical TTCP using other established methods. However, s-TTCP prepared with plasma melting method provides the ideal spherical-shaped TTCP. Moreover, there is a likelihood that the unidentified heat decomposition products in s-TTCP may be converted to TTCP again since the constituents of both s-TTCP and i-TTCP are the same.

In the present study, therefore, thermal treatment was performed to evaluate if heat decomposition products in

s-TTCP could be converted to TTCP without changing its morphology. Then, apatite cement prepared using thermally treated s-TTCP was evaluated in terms of its basic properties and injectability through syringe.

## 2. Materials and methods

### 2.1 Preparation of apatite cement

Spherical tetracalcium phosphate (s-TTCP) particles were prepared at Netsuren Co. (Kanagawa) by plasma melting method using commercially obtained irregular-shaped TTCP (i-TTCP; Taihei Chemical, Osaka). In brief, i-TTCP particle was dropped into reaction vessel filled with Ar where TTCP was melted by the heat generated by plasma. The i-TTCP became spherical due to surface tension, and quenched at room temperature at dropping.<sup>20)</sup> The s-TTCP thus prepared was then supplied for thermal treatment. Thermal treatment was carried out at 1,500°C in an electronic furnace (Super-C; Motoyama Co., Osaka) for four hours and quenched to room temperature. After thermal treatment, slightly aggregated TTCP particles were grounded gently with a mortar and pestle to dissociate the aggregated TTCP. Thermally treated and quenched TTCP was denoted as q-TTCP.

i-TTCP, s-TTCP, and q-TTCP were mixed with dicalcium phosphate anhydrous (DCPA; CaHPO<sub>4</sub>, J. T. Baker Chemical Co., NJ) with a medium particle size of 1.2 μm so that the mixing ratio became equimolar using a mixer (SK-M2; Kyoritsuriko, Tokyo). The mixtures of i-TTCP, s-TTCP, and q-TTCP were denoted as i-AC, s-AC, and q-AC respectively.

It is well known that the liquid phase of AC drastically affects the properties of AC. For example, use of neutral sodium hydrogen phosphate aqueous solution shortens the setting time of AC—whereby this AC is called fast-setting AC (fs-AC).<sup>11),14),17),18)</sup> Use of sodium alginate or other viscous chemicals provides anti-washout ability to AC—whereby this type of AC is called anti-washout AC (aw-AC).<sup>12),14),19),21)-28)</sup> Although aw-AC shows much better handling property and injectability than conventional AC (c-AC) due to the use of a viscous chemical in its liquid phase, we used distilled water for the liquid phase of AC in the present study. This was done so that we could focus on investigating only the effects of powder composition and morphology on the injectability and other basic properties of AC.

The powder phase and the liquid phase—which was distilled water—were mixed with spatula on glass at powder-to-liquid ratio (P/L ratio) of 1.5 to 4.0.

### 2.2 Bulk density measurement

Bulk density of the powder phase of apatite cements was calculated by measuring bulk volume and its weight of apatite cement. In short, 10 cm<sup>3</sup> vessel was filled with apatite cement powder phase and its weight was calculated. Bulk density of the powder phase of apatite cement was calculated by dividing the weight of apatite cement by 10 cm<sup>3</sup>.

### 2.3 Consistency evaluation

Consistency of cement paste was evaluated according to the method set forth in International Standard ISO1566 for dental zinc phosphate cement, in which consistency is defined as the diameter of the spread area of cement paste when a glass plate (140 ± 0.5 g) is placed on 0.5 mL of the paste three minutes after mixing. In the present study, a 2 kg

glass plate was placed on 0.2 cm<sup>3</sup> of cement paste and the spread area measured after three minutes.<sup>14),20),28)</sup>

### 2.4 Injectability evaluation

To obtain the index of injectability of cement paste, a universal testing machine was used to measure the load required to dispense 0.5 cm<sup>3</sup> of paste from 30-mm 18 G syringe needle at a rate of 1 cm<sup>3</sup>·min<sup>-1</sup>.<sup>20)</sup>

### 2.5 Mechanical strength measurement

Mechanical strength of set AC was evaluated in terms of diametral tensile strength (DTS). Cement paste was packed into a splitting cylindrical plastic mold (6 mm in diameter × 3 mm in height). Both ends of the mold were covered by glass plates, clamped, and the paste set by storing in an incubator for 24 hours or up to 30 days at 37°C and 100% relative humidity. The diameter and height of each specimen were measured with a micrometer. Then, samples were crushed at a cross-head speed of 10.0 mm·min<sup>-1</sup> using a universal testing machine (AGS-500A; Shimadzu, Kyoto). The DTS values used were average of at least eight specimens. The bars in Fig. 5 denote standard deviation.

### 2.6 Powder X-ray diffraction (XRD)

Composition of TTCP and set AC was evaluated by means of powder X-ray diffraction (XRD). The XRD patterns of vacuum-dried samples were recorded with a vertically mounted diffractometer system (Rint 2000; Rigaku, Tokyo, Japan) using Ni filtered CuKα generated at 40 kV and 30 mA. Specimens were scanned from 3 to 60° 2θ (where θ is the Bragg angle) in a continuous mode. JCPDS cards 9-0432, 25-1137, and 9-0080 were used as references for HAP, TTCP, and DCPA respectively.

### 2.7 Scanning electron microscopy (SEM)

Morphology of particles before and after spherulization using plasma melting method was observed using scanning electron microscope (SEM) (S-700; Hitachi Co., Tokyo) under an accelerating voltage of 15 kV after gold-coating.

### 2.8 Statistical analysis

For statistical analysis, one-way factorial ANOVA and Fisher's PLSD method as a post-hoc test were performed using "Stat View 4.02" software (Abacus Concepts Inc., Berkeley, California).

## 3. Results

Figure 1 shows the SEM pictures of i-TTCP, s-TTCP, and q-TTCP. As shown, shape of i-TTCP particles was irregular and their surface rugged. In contrast, s-TTCP and q-TTCP made with plasma spray method were spherical and smooth. Basically we found no differences between s-TTCP and q-TTCP.

Figure 2 shows the powder XRD patterns of i-TTCP, s-TTCP, and q-TTCP. Basically, i-TTCP, s-TTCP, and q-TTCP showed the same pattern typical of tetracalcium phosphate. However, we found a small amount of unidentified peaks around 2θ = 22.2 and 22.7 in the case of s-TTCP. The q-TTCP also showed an unidentified peak around 2θ = 22.7, and the height of this peak was similar to that of s-TTCP. However, we found no peaks around 2θ = 37.4 in the case of q-TTCP.

Table 1 summarizes the bulk densities of TTCP and AC

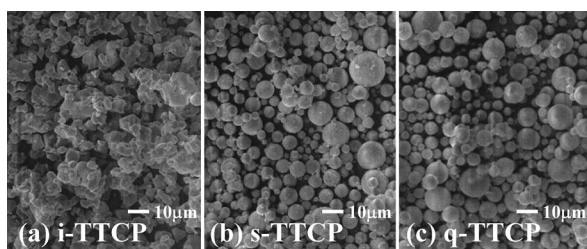


Fig. 1. Typical SEM images of tetracalcium phosphate: (a) i-TTCP; (b) s-TTCP; and (c) q-TTCP.

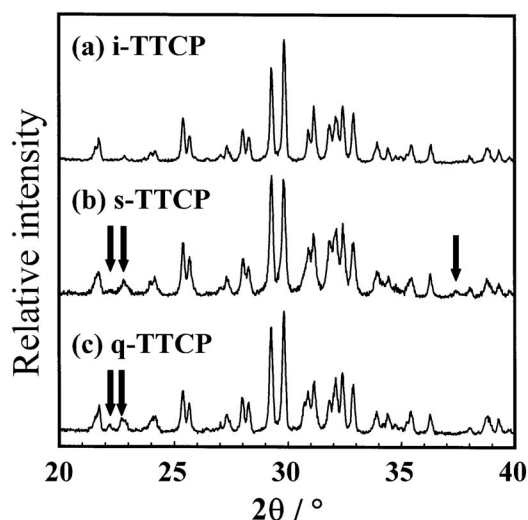


Fig. 2. Powder X-ray diffraction patterns of (a) i-TTCP; (b) s-TTCP; and (c) q-TTCP. Arrows in (b) and (c) indicate unidentified heat decomposition product of TTCP formed during the sphericalization of s-TTCP powder using plasma melting method.

Table 1. Bulk Density of Tetracalcium Phosphate and Apatite Cement

Powder	Bulk density / g·cm <sup>-3</sup>		
	Irregular	Spherical	Quenched
Tetracalcium phosphate	0.96 ± 0.05	1.52 ± 0.06	1.48 ± 0.03
Apatite cement	0.61 ± 0.02	1.13 ± 0.04	1.05 ± 0.057

powders. Bulk density of s-TTCP and q-TTCP were approximately 60% higher than that of i-TTCP. Similarly, bulk density of s-AC and q-AC were approximately 85% higher than that of i-AC. We found no significant differences in bulk density between s-TTCP and q-TTCP or between s-AC and q-AC.

**Figure 3** shows the cement spread area of i-AC, s-AC, and q-AC as a function of P/L ratio. Cement spread area decreased as P/L ratio increased regardless of AC type. When compared at the same P/L ratio, cement spread area of s-AC and q-AC were consistently larger than that of i-AC—regardless of P/L ratio. On the contrary, we found no significant differences in cement spread area between s-AC and

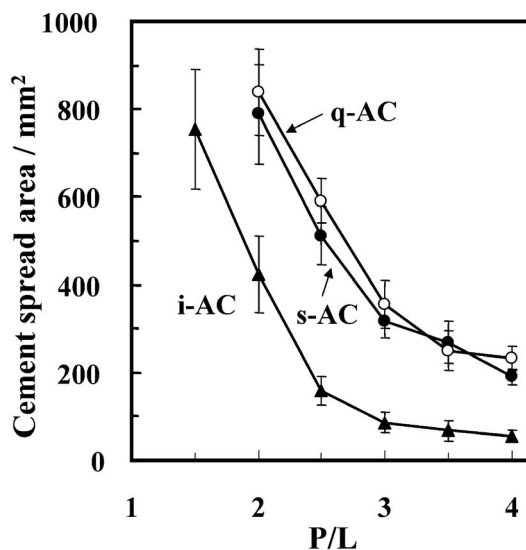


Fig. 3. Comparison of cement spread area as an index of the consistency of cement paste of i-AC, s-AC, and q-AC as a function of powder-to-liquid mixing ratio. ▲, i-AC; ●, s-AC; ○, q-AC.  $n=3$ . Data for i-AC and s-AC are cited from ref [20].

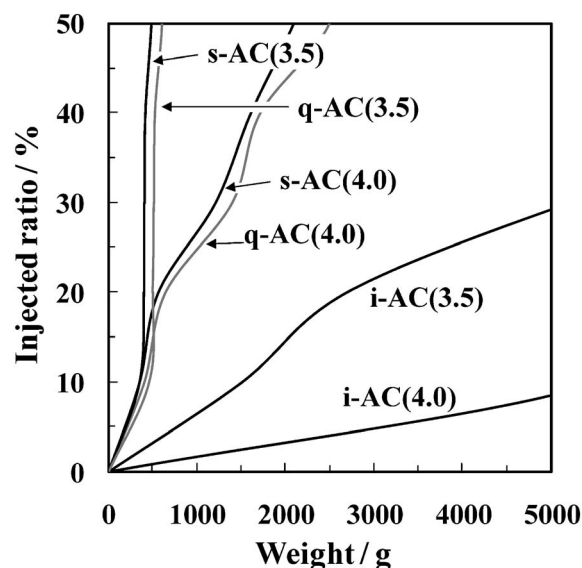


Fig. 4. Injection behaviour of i-AC, s-AC, and q-AC prepared with powder-to-liquid ratios of 3.5 and 4.0. Percentage of injected AC through 30 mm 18 G syringe was plotted against the load required for dispensing.

q-AC regardless of P/L ratio. For example, when P/L ratio was 2.5, cement spread area of s-AC and q-AC were  $512 \pm 67$  mm<sup>2</sup> and  $590 \pm 51$  mm<sup>2</sup>, whereas that of i-AC was  $158 \pm 32$  mm<sup>2</sup>. These results indicated that s-AC and q-AC were vastly superior to i-AC in terms of handling property.

**Figure 4** shows the typical injection profiles of ACs with P/L ratios of 3.5 and 4.0. Larger load was required to inject AC(4.0) than AC(3.5) regardless of AC type. As shown, injection profile of s-AC and q-AC were similar regardless of P/L ratio. In contrast, larger load was required to inject i-AC than s-AC or q-AC at the same P/L ratio.

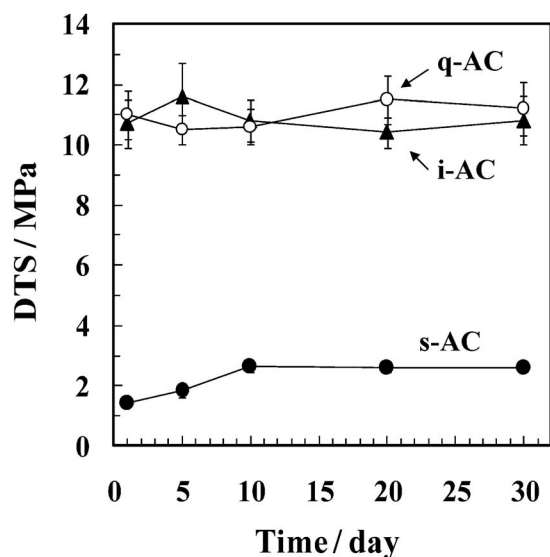


Fig. 5. Evaluation of diametral tensile strength (DTS) versus incubation time for i-AC, s-AC, and q-AC. ▲, i-AC; ●, s-AC; ○, q-AC. Powder-to-liquid mixing ratio was 3.5.  $n=8$ . Data for i-AC and s-AC are cited from ref. [20].

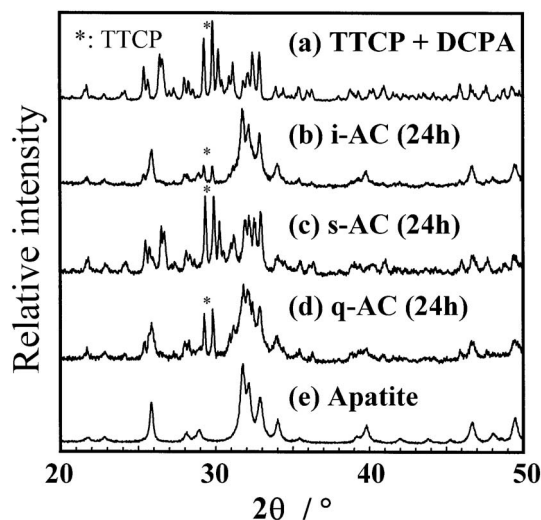


Fig. 6. Powder X-ray diffraction patterns of (a) powder phase of i-AC, i.e., equimolar mixture of TTCP and DCPA; (b) set i-AC; (c) set s-AC; (d) set q-AC; and (e) commercially obtained hydroxyapatite.

Figure 5 summarizes the DTS value of i-AC, s-AC, and q-AC as a function of incubation time. As shown in this figure, DTS value of i-AC and q-AC were much higher ( $p < 0.01$ ) than s-AC regardless of incubation time. DTS value of i-AC and q-AC were the same regardless of incubation time. DTS value of s-AC increased with incubation time up to 10 days, then remained constant at the same DTS value. In contrast, we found no significant increases in incubation time for i-AC and q-AC.

Figure 6 summarizes the XRD patterns of (a) powder phase of i-AC, i.e., an equimolar mixture of i-TTCP and DCPA; (b) set i-AC; (c) set s-AC; and (d) set q-AC. XRD

pattern of (e) crystalline HAP is also listed for comparison. In (b), (c), and (d), powder phase and liquid phase of AC were mixed at powder-to-liquid ratio of 3.5, and left to set in an incubator at 37°C and 100% relative humidity for 24 hours. Set i-AC showed the typical apatitic patterns with small amount of unreacted TTCP. In contrast, we found limited amount of apatite formation in set s-AC and larger amount of unreacted TTCP and DCPA.

#### 4. Discussion

Results obtained in this study demonstrated clearly that thermal treatment was very effective in converting heat decomposition products in s-TTCP, which were formed during plasma melting method, to TTCP without changing its morphology. In connection with injectability and handling property, it is very important that the morphology of cement paste is not changed by thermal treatment. As shown in Fig. 1, no morphological changes were observed after s-TTCP was subjected to thermal treatment. As a result, handling property and injectability of q-AC were almost the same as those of s-AC, and much better than those of i-AC. For example, when powder-to-liquid mixing ratio was 2.5, cement spread area of i-AC was  $158 \pm 32 \text{ mm}^2$  whereas that of s-AC and q-AC were  $512 \pm 68 \text{ mm}^2$  and  $591 \pm 51 \text{ mm}^2$  respectively. This indicated that s-AC and q-AC spread approximately three to four times more than i-AC when the same load was applied to spread the ACs. Similarly, injection from the syringe was much easier in s-AC and q-AC than in i-AC.

On the other hand, we found compositional changes in s-TTCP after thermal treatment. As shown in Fig. 2, heat decomposition products were formed after s-TTCP was prepared using plasma melting method. Although the heat decomposition products could not be identified due to their limited amount, one of the heat decomposition products might be calcium oxide—which showed its highest XRD peak around  $2\theta = 37.4$ . Unfortunately, it was impossible to detect the second and third strong peaks corresponding to calcium oxide, namely  $2\theta = 53.9$  and  $32.2$ . Moreover, peaks around  $2\theta = 22.2$  and  $22.7$  could not be identified. In summary, although the composition of heat decomposition products could not be identified, thermal treatment was at least very effective in converting some heat decomposition product to TTCP. As shown in Fig. 2(c), unidentified peak around  $2\theta = 37.4$ —which was seen in s-TTCP—disappeared after thermal treatment. Unfortunately, thermal treatment employed in the present study could not convert all heat decomposition products to TTCP. In other words, heat decomposition products that showed XRD peaks around  $2\theta = 22.2$  and  $22.7$  remained as they were even after thermal treatment.

Nonetheless, q-AC—a mixture of q-TTCP and DCPA set to form apatite as shown in Fig. 6—exhibited much higher mechanical strength similar to i-AC as shown in Fig. 5. However, transformation to apatite might not be complete in the case of q-AC. As shown in Fig. 6, large amount of TTCP remained unreacted in the case of q-AC as compared to i-AC. Although transformation to apatitic mineral was limited, q-AC showed basically the same mechanical strength as i-AC (Fig. 5). It is well known that conversion to apatitic mineral brings about a higher mechanical strength in AC.<sup>(11), (13), (18)</sup> In this connection, q-AC was expected to show lower mechanical strength than i-AC. Although the detailed

mechanism has not been clarified in the present study, the similarity in mechanical strength might in part be due to the higher density of set cement. As shown in Table 1, bulk density of q-AC was higher than that of i-AC, and it is known that bulk density of apatite cement has close relationship with its mechanical strength.<sup>13)</sup> Therefore, the higher density of q-AC could have compensated for the limited transformation to apatitic mineral, thus resulting in similar mechanical strength with i-AC.

It should be noted that there are many methods to prepare spherical TTCP. Unfortunately, the q-TTCP preparation method employed in the present study is expensive and time-consuming. This is because s-TTCP has to be prepared first by plasma melting method, followed by thermal treatment to obtain ideal spherical-shaped TTCP. On this note, other spherical TTCP preparation methods should likewise be evaluated as we continue to investigate how to further eliminate heat-decomposed TTCP from s-TTCP prepared by plasma melting method.

### 5. Conclusion

It was found that some heat decomposition products in s-TTCP converted to TTCP when s-TTCP was heated at 1,500°C for four hours and quenched at room temperature (q-TTCP) without changing its morphology. Therefore, AC containing q-TTCP showed excellent On the other hand, conversion of heat decomposed product to TTCP result in the transformation of AC containing q-TTCP to apatitic monolith and showed equivalent mechanical strength similar to AC that contained i-TTCP. Based on these findings, we concluded that AC containing q-TTCP would benefit patients since it delivered excellent injectability without sacrificing basic setting properties of AC.

**Acknowledgments** This study was supported in part by a grant-in-aid for Scientific Research from the Ministry of Education, Science, Sports, and Culture.

### References

- 1) G. Pasquier, B. Flautre, M. C. Blary, K. Anselme and P. Hardouin, *J. Mater. Sci.: Mater. Med.*, **7**, 683-690 (1996).
- 2) G. Daculsi, *Biomaterials*, **19**, 1473-1478 (1998).
- 3) A. Dupraz, T. P. Nguyen, M. Richard, J. Delecrin and G. Daculsi, *J. Mater. Sci.: Mater. Med.*, **7**, 52-55 (1996).
- 4) W. E. Brown and L. C. Chow, "Paste as mineralizers and cements" (U.S. Patent, No. 4, 612, 053, 1986).
- 5) W. E. Brown and L. C. Chow, "Cements Research Progress", Ed. by P. W. Brown, American Ceramic Society, Westerville (1987) pp. 351-379.
- 6) B. R. Constantz, I. C. Ison, M. T. Fulmer, R. D. Poser, S. T. Smith, M. VanWagoner, J. Ross, S. A. Goldstein, J. B. Jupiter and D. I. Rosenthal, *Science*, **267**, 1796-1799 (1995).
- 7) F. C. M. Driessens, M. G. Boltong, O. Bermudez and J. A. Planell, *J. Mater. Sci.: Mater. Med.*, **4**, 503-508 (1993).
- 8) F. C. M. Driessens, M. G. Boltong, O. Bermúdez, J. A. Planell, M. P. Ginebra and E. Fernández, *J. Mater. Sci.: Mater. Med.*, **5**, 164-170 (1994).
- 9) R. I. Martin and P. W. Brown, *J. Mater. Sci.: Mater. Med.*, **6**, 138-143 (1995).
- 10) K. Kurashina, H. Kurita, M. Hirano, J. M. A. de Blicke, C. P. A. T. Klein and K. de Groot, *J. Mater. Sci.: Mater. Med.*, **6**, 340-347 (1995).
- 11) K. Ishikawa, S. Takagi, L. C. Chow and Y. Ishikawa, *J. Mater. Sci.: Mater. Med.*, **6**, 528-533 (1995).
- 12) K. Ishikawa, Y. Miyamoto, M. Kon, M. Nagayama and K. Asaoka, *Biomaterials*, **16**, 527-532 (1995).
- 13) K. Ishikawa and K. Asaoka, *J. Biomed. Mater. Res.*, **29**, 1537-1543 (1995).
- 14) K. Ishikawa, Y. Miyamoto, M. Takechi, Y. Ueyama, K. Suzuki, M. Nagayama and T. Matsumura, *J. Biomed. Mater. Res.*, **44**, 322-329 (1999).
- 15) P. D. Costantino, C. D. Friedman, K. Jones, L. C. Chow, H. J. Pelzer and G. A. Sisson, *Arch. Otolaryngol. Head Neck Surg.*, **117**, 379-384 (1991).
- 16) C. D. Friedman, P. D. Costantino, K. Jones, L. C. Chow, H. J. Pelzer and G. A. Sisson, *Arch. Otolaryngol. Head Neck Surg.*, **117**, 385-389 (1991).
- 17) Y. Miyamoto, K. Ishikawa, M. Takechi, T. Toh, Y. Yoshida, M. Nagayama, M. Kon and K. Asaoka, *J. Biomed. Mater. Res.*, **37**, 457-464 (1997).
- 18) Y. Miyamoto, K. Ishikawa, H. Fukao, M. Sawada, M. Nagayama, M. Kon and K. Asaoka, *Biomaterials*, **16**, 855-860 (1995).
- 19) Y. Miyamoto, K. Ishikawa, M. Takechi, M. Yuasa, M. Kon, M. Nagayama and K. Asaoka, *Biomaterials*, **17**, 1429-1435 (1996).
- 20) K. Ishikawa, S. Matsuya, M. Nakagawa, K. Udoh and K. Suzuki, *J. Mater. Sci.: Mater. Med.*, **15**, 13-17 (2004).
- 21) Y. Ueyama, K. Ishikawa, T. Mano, T. Koyama, T. Matsumura and K. Suzuki, *J. Biomed. Mater. Res.*, **55**, 652-660 (2001).
- 22) S. Tajima, N. Nishimoto, Y. Kishi, S. Matsuya and K. Ishikawa, *Dent. Mater. J.*, **23**, 329-334 (2004).
- 23) Y. Shiga, R. Shimogoryo, T. Oka, S. Matsuya and K. Ishikawa, *Dent. Mater. J.*, **23**, 335-339 (2004).
- 24) L. Leroux, Z. Hatim, M. Freche and J. L. Lacout, *Bone*, **25**, 31S-34S (1999).
- 25) P. Iooss, A. M. Le Ray, G. Grimandi, G. Daculsi and C. Merle, *Biomaterials*, **22**, 2785-2794 (2001).
- 26) M. P. Ginebra, A. Rilliard, E. Fernandez, C. Elvira, J. San Roman and J. A. Planell, *J. Biomed. Mater. Res.*, **57**, 113-118 (2001).
- 27) M. Takechi, Y. Miyamoto, K. Ishikawa, M. Yuasa, M. Nagayama, M. Kon and K. Asaoka, *J. Mater. Sci.: Mater. Med.*, **7**, 317-322 (1996).
- 28) Y. Miyamoto, K. Ishikawa, M. Takechi, T. Toh, T. Yuasa, M. Nagayama and K. Suzuki, *Biomaterials*, **19**, 707-715 (1998).